Received: 22 July 2019 | Accepted: 25 July 2019

DOI: 10.1002/mdp2.101

REPORT

WILEY

Application of hot isostatic pressing (HIP) technology to diffusion bond refractory metals for proton beam targets and absorbers at CERN

Josep Busom Descarrega[1] | **Marco Calviani**[1] | **Thomas Hutsch**[2] | **Edmundo López Sola**[1] | **Ana Teresa Pérez Fontenla**[1] | **Antonio Perillo Marcone**[1] | **Stefano Sgobba**[1] | **Thomas Weißgärber**[2]

[1] European Organization for Nuclear Research (CERN), Geneva, Switzerland

[2] Fraunhofer Institute for Manufacturing Technology and Advanced Materials IFAM, Dresden, Germany

Correspondence
J. Busom Descarrega, European Organization for Nuclear Research (CERN), Route de Meyrin, CH-1211, Geneva 23, Switzerland.
Email: josep.busom.descarrega@cern.ch

Abstract

A target assembly, composed of several collinear molybdenum (Mo)-based and tungsten (W)-based cylindrical blocks, will reside in the core of the new beam dump facility (BDF) being designed at the European Laboratory for Particle Physics (CERN). The target blocks will be protected from the cooling water erosion-corrosion by a tantalum (Ta)-based cladding.

In order to obtain intimate and reliable bonding between the several cylinders composing each target block and with the cladding, hot isostatic pressing (HIP) assisted diffusion bonding technique was explored. Several down-scaled target block prototypes were conceived to investigate the bondings. Starting from the previously gained experience in Ta cladding on W from neutron spallation targets, here, we present results on Ta cladding on TZM (Mo alloy), Ta2.5W (Ta alloy) cladding on TZM and W, and on TZM to TZM and W to W self-bondings. The resulting interfaces were systematically characterized with electron microscopy, tensile testing, and thermal conductivity measurements.

Successful diffusion bonding was achieved for all the studied material combinations, resulting in homogeneous and defect-free interfaces, strong interfacial bondings, and limited interfacial thermal contact resistance. The HIP parameters and diffusion interfacial aids were of great importance to optimize the interface and bulk material properties.

KEYWORDS

adhesion strength, bonded joints, heat treatment, lap joint, materials testing, mechanical properties of weldments, microstructure, tensile test

[The copyright line for this article was changed on 14 October 2019 after original online publication.]

1 | INTRODUCTION

In the framework of the Physics Beyond Colliders initiative at the European Laboratory for Particle Physics (CERN), a new infrastructure named beam dump facility (BDF) has been proposed to study the Hidden Sector. The new facility is to be located in a new experimental complex at the Super Proton Synchrotron (SPS) at CERN. A first proposed experiment to employ this infrastructure is the Search for Hidden Particles (SHiP).[1]

The new BDF production target has to cope with two main objectives: On the one hand, as a beam absorber, it should contain most of the cascade generated by the interaction with the 400 GeV SPS proton beam; on the other hand, as a target, it should maximize the production of secondary particles from the interaction of the primary proton beam and the dump material, such as charmed mesons and photons.[2]

The BDF production target will be based on a solid state target made of high Z materials with short interaction length to maximize the production of charmed mesons required by the experiment.

The actual BDF production target design, shown in Figure 1, consists of 18 collinear TZM (Mo alloy with 0.5 wt% titanium, 0.08 wt% zirconium, and 0.03 wt% carbon) and tungsten (W) cylinders with a diameter of 250 mm and variable lengths, from 25 to 350 mm, for a total effective target length of around 1.3 m. The target requires active cooling to dissipate the deposited power. Cooling is carried out by a continuous flow of demineralized water, circulating around the target and through the 5-mm gaps between the blocks.[3]

For both target materials, multidirectionally forged blocks are considered due to the isotropic microstructure and superior mechanical properties provided by this manufacturing process. The available dimensions for this material grade are limited and might compromise the supply of the biggest W target cylinders.* Thus, it was considered to diffusion-bond coaxially several multidirectionally forged cylinders to reach the desired target block length.

W and TZM feature limited corrosion resistance in high temperature flowing water.[4] Moreover, in irradiation environments, corrosion rates of both materials increase significantly due to the build-up of water radiolysis products.[5,6] Materials such as Zircaloy, stainless steels, titanium alloys, and tantalum (Ta) alloys exhibit excellent corrosion resistance in aqueous environments.[7]

Covering the target material with a 1- to 2-mm-thick layer of the latter materials is proposed as a practical solution to protect the target core without reducing the target physics performance.[8-10]

Ta was firstly considered as cladding material for the extensive experience in other facilities.[8,10,11] Ta2.5W (Ta alloy with 2.5 wt% of W) was also considered due to the superior mechanical properties, corrosion resistance, and radiation resistance compared with Ta.[12,13]

The protective layer requires intimate bonding to the target materials in order to ensure the maximal power evacuation to the coolant.

Ta-based materials feature perfect mutual solubility with Mo and W, avoiding intermetallic phases at the resulting bondings. Moreover, they feature similar thermal expansion than the target materials, hence minimizing the interfacial stress during the target thermal cycles.

Diffusion bonding between the target materials (W to W and TZM to TZM) has been reported in literature for simple geometries such as single or double lap joints via uniaxial diffusion bonding techniques. Interfacial aids resulted mandatory to achieve diffusion bonding for W to W and to reach 100% joint efficiency for TZM to TZM.[14,15]

The most promising technique to diffusion bond the cladding to the target materials is hot isostatic pressing (HIP) assisted diffusion bonding. The utilization of this technique to clad Ta was firstly reported to protect a water cooled W target at ISIS[11] and was lately further developed and applied in the construction of neutron spallation targets at KENS[8,16] and at LANSCE.[10,17] HIP allows application of higher bonding pressures than other diffusion bonding techniques. Thus, lower bonding temperatures can be employed to avoid recrystallisation and grain growth phenomena in the base materials.

This work copes with multiple objectives. First is to explore for the first time the HIP assisted diffusion bonding between several target material cylinders (W to W and TZM to TZM). Second is to validate the HIP assisted diffusion bonding between all the cladding and target candidate materials for BDF, especially for the TZM and Ta2.5W, where no studies are reported.

In parallel, there is also an interest to study the effects of using diffusion interfacial aids and to explore the effect of different HIP cycles on the interfaces and bulk materials properties.

Several studies dedicated efforts on improving prototype preparation routines, solving surface state related problems, and ameliorating the interface between cladding and target.[8,10] The prototype preparation routine was optimized in

*A total of 250 mm diameter and longer than roughly 150 mm in length.

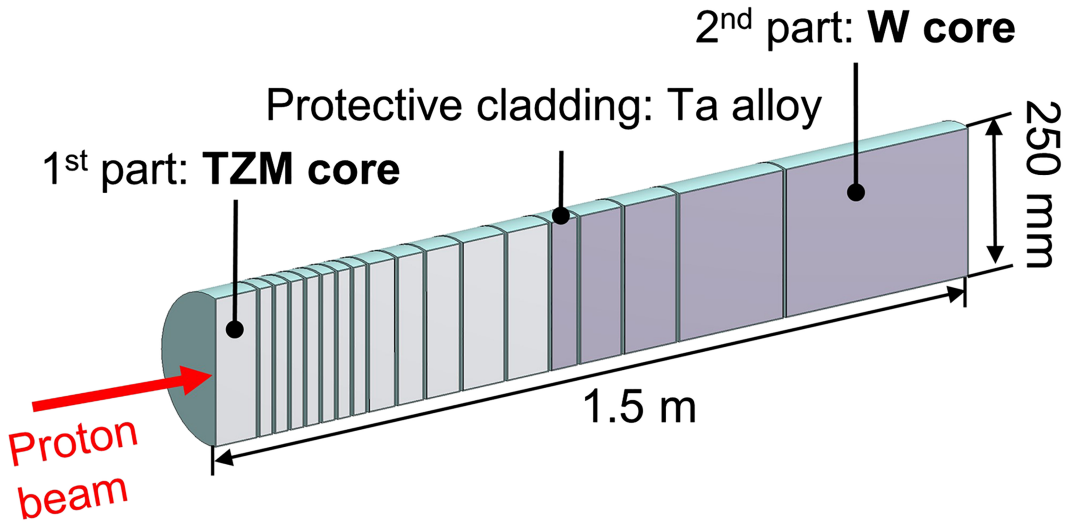

FIGURE 1 3D cross-sectional cut view of the BDF final target design, showing the TZM part as well as the W one, both clad with a Ta-alloy

previous internal studies, and no surface-related problems are encountered in this work. Therefore, this study is specifically addressed to the diffusion bonded interfaces.

2 | EXPERIMENTAL WORK

2.1 | Prototypes configuration and materials

Several prototypes were fabricated to study the diffusion bonded interfaces. The prototypes were conceived with geometries scaled to those of the target blocks to already anticipate any potential issue derived from the target geometry.

Four materials were employed in the fabrication of the prototypes, W and TZM as target materials and Ta and Ta2.5W as cladding materials.

The prototypes were built using one or two cylinders of the target material. The cylinders were fitted inside a tube of cladding material and closed from the two sides by two covers, also from cladding material. The cladding material's thickness was of 1.5 mm in the cylindrical part, but it was increased to 10 mm for the two covers to allow the extraction of bigger bonding specimens, required for mechanical testing. The bonding of the cladding material to the target material was created by HIP, as described hereafter.

Two types of prototypes were built, either with a single or double target material cylinders. The single-cylinder prototypes were produced to study the target to cladding materials bonding whilst the double-cylinder prototypes were produced to study the target to target materials bonding. Ta foils were eventually introduced between the materials as diffusion interfacial aids. The foils' thickness was fixed in 50 mm, following literature recommendations, to maximize the bonding strength.[14,18] The two types of prototypes are represented in Figure 2 with their respective components.

W was supplied by Plansee in the form of forged and annealed 25- and 50-mm diameter rods, with a minimal density of 99.97% and a hardness of 420 to 480 HV. TZM was also supplied by Plansee in form of forged and annealed 25- to 50-mm diameter rods, with a hardness of 250 to 310 HV. Ta and Ta2.5W were supplied by Plansee and WHS Sondermetalle respectively, both in the form of plates, seamless tubes, and foils, all products in the annealed state. All the materials employed in this study did not undergo further specific surface preparation than conventional machining.

2.2 | Manufacturing of prototypes

Before the assembly of each prototype, the target material cylinder and the two cladding material covers were machined to a diameter 100 μm smaller than the tube. This tolerance allowed sufficient spacing for the introduction of the target material cylinder but narrow enough to avoid cladding corrugation during the HIP cycle.

A continuous and hermetic (gas tight) cladding material capsule covering the target material cylinder was required to ensure the application of isostatic pressure on the cladding materials during the HIP cycle. With this aim, electron beam

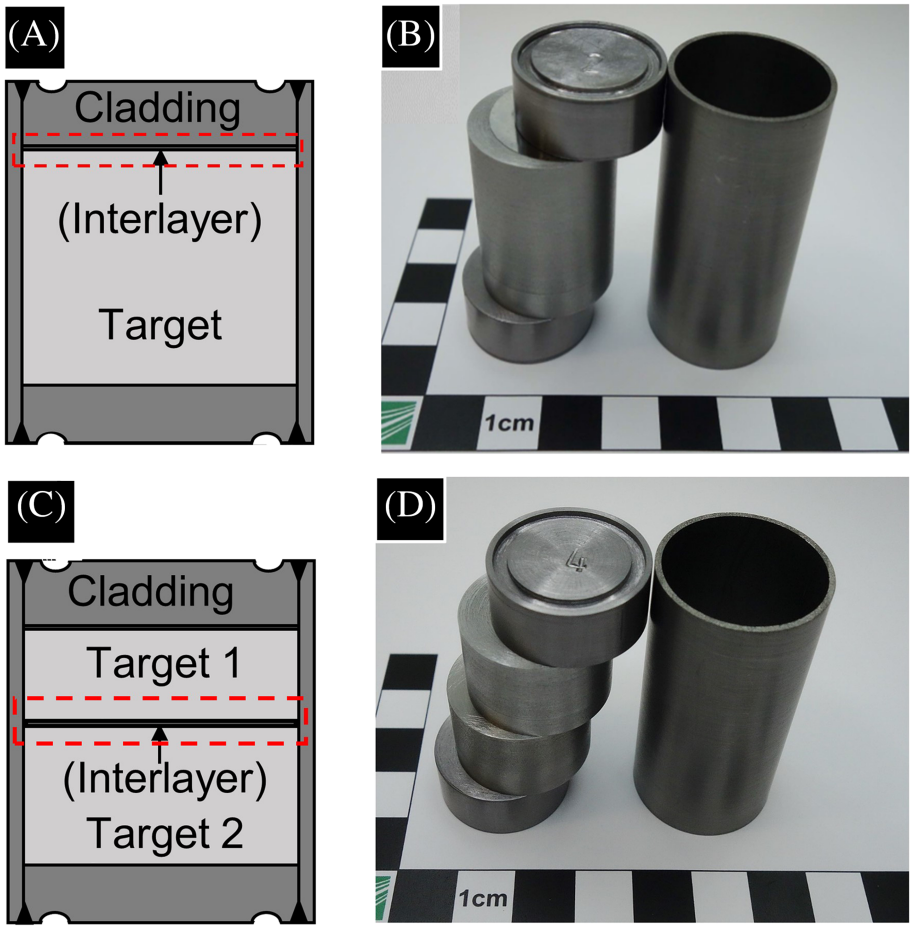

FIGURE 2 A, Cross-sectional schematic of the prototypes designed to study the target to cladding materials bonding, with the specimen extraction area outlined in red. B, Image of the target to cladding materials prototype components before assembly. C, Cross-sectional schematic of prototypes designed to study the target to target materials bonding, with the specimen extraction area outlined in red. D, Image of the target to target materials prototype components before assembly

welding was employed to weld the tube and both covers of each prototype. A corner-flange–type weld was carried out to maintain the heat affected zone far from the cladding-target materials interface. The air between the cladding and target materials was evacuated before welding by placing the prototypes under vacuum. After the welding operation (see Figure 3A), each prototype was helium leak tested to ensure the tightness of the cladding material capsules.

A HIP cycle was carried out on the prototypes to diffusion bond the cladding material to the target material and eventually the target to target materials too. A HIP furnace with high purity Argon as pressurized gas and a Mo heater were employed to minimize the atmospheric impurities which could potentially be absorbed by the cladding surface. Additionally, the prototypes were wrapped with Ta and Zr foils (see Figure 3B) to capture all the remaining impurities.[8]

The heating rate during the HIP cycle was of 10 K/min, and the dwell time at the nominal temperature and pressure was 3 hours. In this work, two HIP cycle parameters were tested: 1200°C and 150 MPa (from now on referred as "L"), in which temperature was maintained below the W and TZM recrystallisation temperature, in order to preserve a fine microstructure in the target materials; 1400°C and 200 MPa (from now on referred as "H") in which temperature was raised above the W and TZM recrystallisation temperature in order to obtain the best diffusion bonding even if target material bulk properties were partially sacrificed.[19]

2.3 | Target prototypes characterization

After the HIP cycle (see Figure 3C), electro discharge machining (EDM) was employed to extract interface specimens from the prototypes, as shown in and Figure 3D. The target to cladding materials interface specimens was extracted from the single cylinder prototypes (shown in Figure 2A,B), and the target to target material interface specimens was extracted from the double cylinder prototypes (shown in Figure 2C,D).

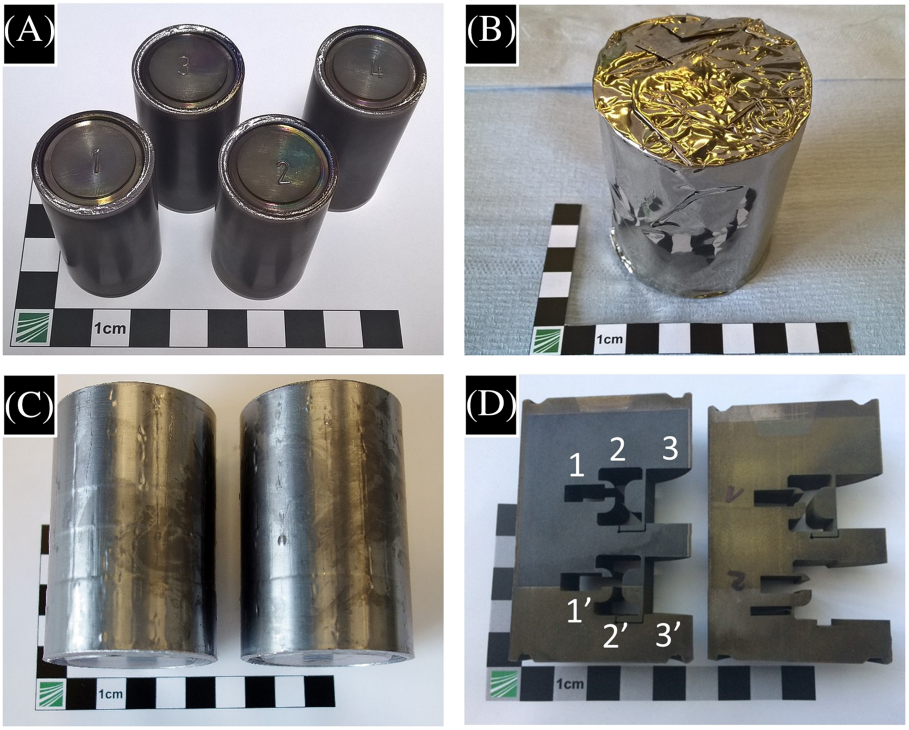

FIGURE 3 A, Picture of four prototypes after welding of the Ta/Ta2.5W capsule. B, Picture of one prototype after welding and wrapped with the getter foils before the HIPing cycle. C, Picture of two prototypes after the HIPing cycle and removal of the getter foils. Cladding deformation and corrugation is appreciable. D, Picture of two half prototypes after cross-sectional cut with EDM. Specimen extraction can be appreciated in 1,2,3 for target to target materials bonding and 1′, 2′, 3′ for cladding to target materials bonding. Specimens "1" were dedicated for thermal conductivity measurements, specimens "2" for tensile testing and specimens "3" for interface microscopy

Specimens at the interface level were prepared by conventional mechanical grinding and polishing to allow interface imaging. Micrographs were acquired employing a scanning electron microscope (SEM) Zeiss EVO 50 XVP with an accelerating voltage of 15 kV, a current of 300 pA, and an operating distance of 8 mm.

Tensile testing was carried out on nonstandard miniaturized tensile specimens of 4 mm^2 section. When measuring the bonded interfaces' strength, the interface was coincident with the minimal specimen section. Due to the small specimen gauge length, elongation could not be precisely measured and only the tensile strength values are reported. A minimum of three specimens were tested for each type of bonding. Testing was carried out employing a tensile testing Zwick 1476 system and a speed of 0.07 mm/min.

Hardness measurements were carried out employing a Falcon 500 system from INNOVATEST with a vickers indenter and a load of 5 N (HV5).

The thermal conductivity was indirectly measured by employing Equation (1):

$$\lambda = \alpha \times C_p \times \rho, \tag{1}$$

where α is the measured thermal diffusivity, C_p is the heat capacity, and ρ is the density. The α was measured using Xenon pyrometry "Nanoflash" from Netzsch. The C_p was characterized using "DSC204 Phoenix" from Netzsch. The ρ was determined by the Archimedes method.

The number of prototypes built for this study was determined in order to obtain all the combinations between target materials to cladding materials, target to target materials, the use of Ta interlayer, and HIP cycles. The list of all the specimens under study resulting from these combinations is given in Table 1.

3 | RESULTS

3.1 | Target-target materials bonding

The bonding interfaces between target materials are observable from the SEM micrographs given in Figure 4. The interfaces showed incomplete diffusion bonding when no interlayer was used: The interface between TZM and TZM showed

TABLE 1 List of the specimens studied in this work with the corresponding target and cladding materials, eventual use of interlayer, and employed HIP cycle

Bonding Specimen Number	Target to Cladding			
	Target Material	**Cladding Material**	**Interlayer**	**HIP**
1	TZM	Ta2.5W	x	L
2			-	
3		Ta	-	
4	W	Ta2.5W	x	
5			-	
6		Ta	-	
7	TZM	Ta2.5W	x	H
8			-	
9		Ta	-	
10	W	Ta2.5W	x	
11			-	
12		Ta	-	
	Target to Target			
	Target Material 1	**Target Material 2**	**Interlayer**	**HIP**
13	TZM	TZM	-	L
14			x	
15	W	W	-	
16			x	
17	TZM	TZM	x	H
18	W	W	x	

[Correction added on 14 October 2019, after first online publication: Table 1 has been corrected.]

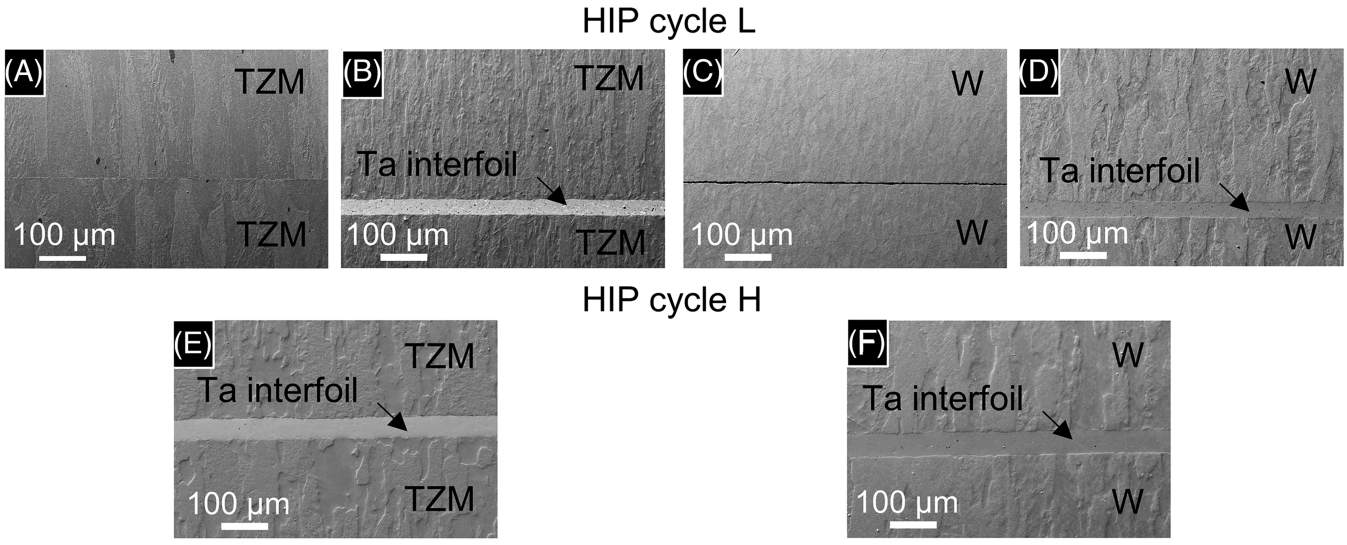

FIGURE 4 Secondary electron micrographs at the interface level for the target to cladding specimens at 150× magnifications. Note that specimen (C) did not present any apparent bonding

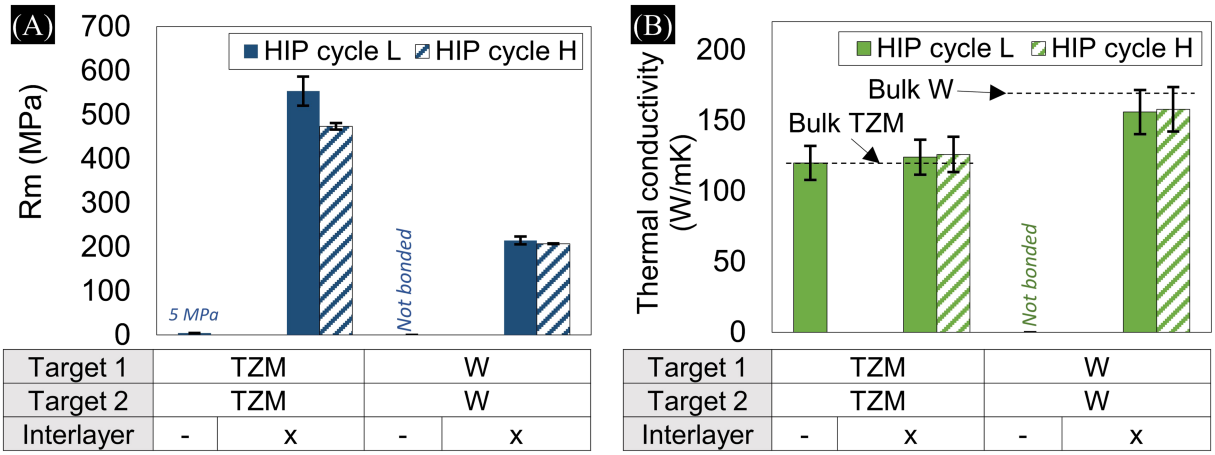

FIGURE 5 A, Average tensile strength for each type of bonding between target and target materials. B, Thermal conductivity for each type of bonding between target and target materials. Bulk materials thermal conductivity are reported as reference
[Correction added on 14 October 2019, after first online publication: Figure 5 has been corrected.]

recurrent gaps and the interface between W and W does not show any apparent bonding. The interfaces between target materials with an interlayer indicated potential complete diffusion bonding: interfaces were in continuous contact with no features such as heterogeneities, gaps, or retained porosity. Difficulties were encountered to image the diffusion layers due to specimen preparation artefacts but also due to the small layer thickness, which was approximately 1 μm when appreciable.

The tensile strength of the target to target material interface is given in Figure 5A. The bonding for the interfaces without interlayer featured low strength values, with 5 MPa between TZM and TZM and no mechanical bonding between W and W. However, when using an interlayer, strong bonding was exhibited. Specimens between TZM and TZM (550 MPa) featured higher strength than between W and W (215 MPa). The strength of the bonding was found to be slightly lower for the HIP cycle "H".

The thermal conductivity was measured across the target to target materials interface and is given in Figure 5B. All the specimens featuring bonding showed thermal conductivities equal to bulk thermal conductivity, indicating an absence of interface contact resistance independently of the bonding parameters. No clear tendencies were observed between either the use of interlayer or the HIP cycle and the thermal conductivity.

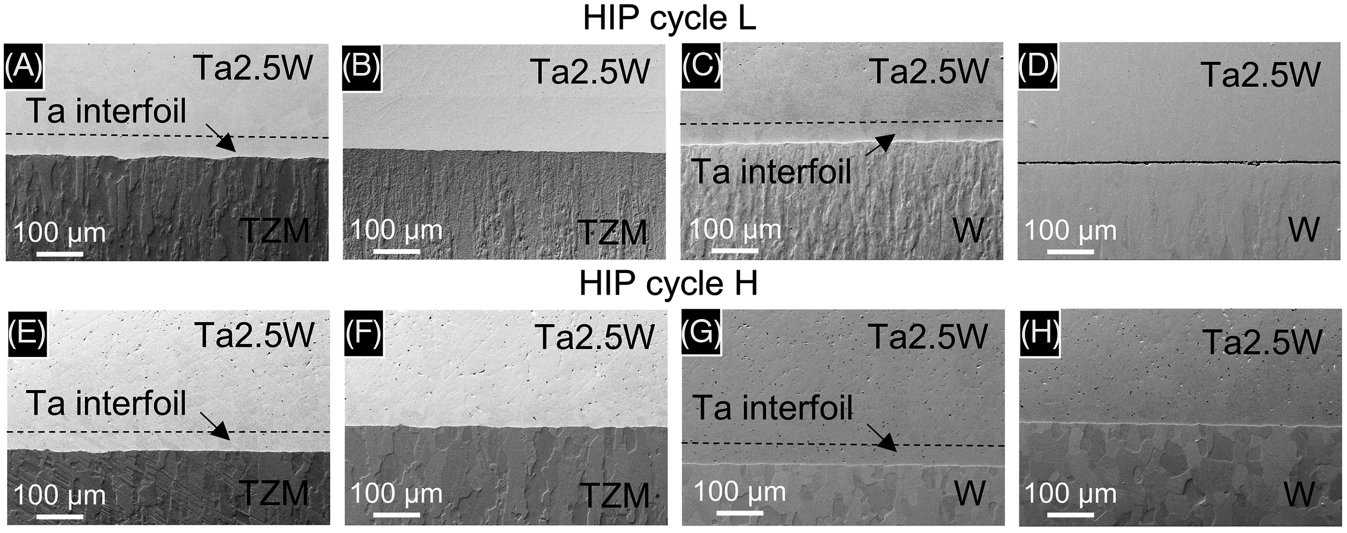

FIGURE 6 Secondary electron micrographs at the interface level for the target to target material specimens under study at 150× magnifications. Note that specimen (D) did not present any apparent bonding

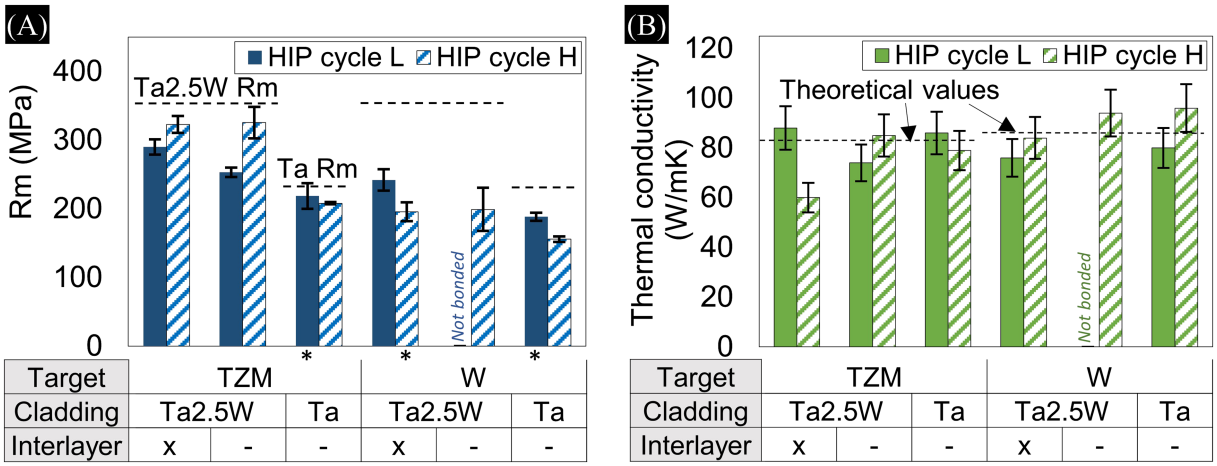

FIGURE 7 A, Average tensile strength for each type of bonding between cladding and target materials. Ta2.5W and Ta tensile strength reported as reference. Specimens marked with * failed outside the gauge length. B, Thermal conductivity for each type of bonding between cladding and target materials. Theoretical thermal conductivity without interface resistance reported as reference
[Correction added on 14 October 2019, after first online publication: Figure 7 has been corrected.]

3.2 | Target-cladding materials bonding

The interfaces between target and cladding materials are observable in the SEM micrographs given in Figure 6. Nearly all the specimens showed interfaces in which the two materials are in perfect contact, indicating potential diffusion bonding. Only the specimens between W and Ta2.5W with HIP cycle "L" did not show apparent bonding (see Figure 6D). In general terms, the interfaces did not present any heterogeneity, gaps, or retained porosity. However, some micrometer-sized porosities were observed in the interfaces between the Ta interlayer and Ta2.5W for the specimens with HIP cycle "L". The diffusion layer was not discernible as in the target to target materials bondings.

The tensile strength of the interfaces is given in Figure 7. Both cladding materials present lower strength than the target materials; thus, all the interface tensile strengths are limited by the latter. The tensile strengths of the cladding materials were 360 MPa for Ta2.5W and 220 MPa for Ta, respectively. Most part of the bonding specimens failed at the interface level, therefore measuring the interface strength. However, some specimens failed at the base material, and therefore, the interface strength might be greater.

Strong bonding with 100% joint efficiency was achieved for the combinations between TZM-Ta2.5W (330 MPa), TZM-Ta (215 MPa), and W-Ta (185 MPa). Nevertheless, for the couple W-Ta2.5W (230 MPa), the highest achieved joint efficiency was 70%.

For TZM as target material, the strongest bonding was reached with Ta2.5W as cladding material and the HIP cycle "H," independently on the use of Ta foil. For W as target material, the highest bonding strength was achieved with Ta2.5W as cladding material but required the use of the Ta interlayer. Stronger bonding was always achieved for the HIP cycle "L."

Interlayers increased the bonding strength only in the case of Ta2.5W bonding to W and for the "L" cycle. In all the other combinations, the Ta interlayer affected negatively the bonding strengths. Nevertheless, the use of the Ta interlayer was the only option to obtain a successful bonding W to Ta2.5W with the HIP cycle "L." On the one hand, the HIP cycle with higher temperature increased the bonding strength for the Ta2.5W claddings. On the other hand, the higher temperature cycle reduced the bonding strength for the Ta claddings.

Thermal conductivity was measured across the cladding to target materials interface and is given in Figure 7. Values are compared with the theoretical thermal conductivities, calculated with the thermal resistance law, assuming no interface contribution to the total thermal resistance. The theoretical thermal conductivity for the couples W-Ta and W-Ta2.5W is 85 W/mK, and for the couples TZM-Ta and TZM-Ta2.5W, it is 82 W/mK.

From all the specimens featuring apparent bonding, only the specimens between TZM-Ta2.5W with interlayer and HIP cycle "H" showed significant reduced thermal conductivity: 73% with respect to the theoretical one. For all the other specimens, thermal conductivity values were close or equal to the theoretical values. No clear tendencies were observed between the thermal conductivity and the studied variables.

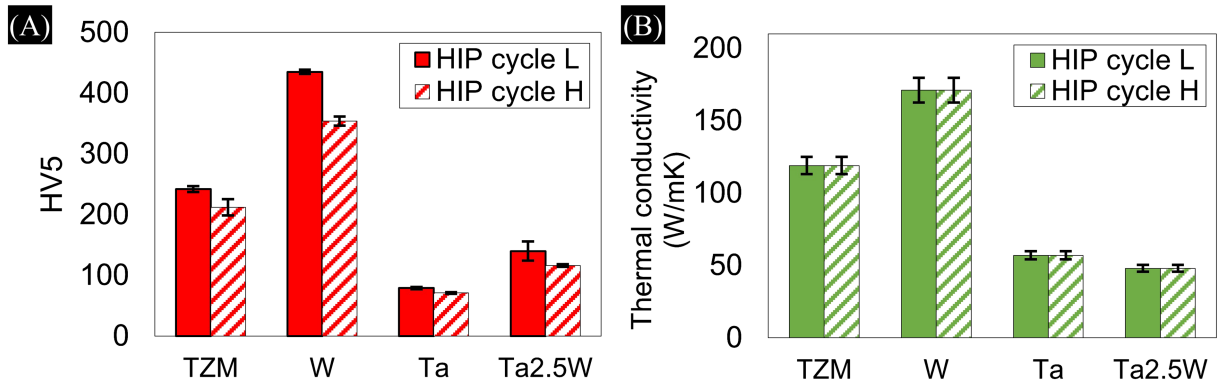

FIGURE 8 A, HV5 micro-hardness and B, thermal conductivity values for the four materials after the respective HIP cycles

3.3 | Bulk material

Additional hardness and thermal conductivity measurements were carried out on bulk material specimens from the prototypes to evaluate the effect of the HIP cycles on the material properties.

The microstructure of the TZM and W was appreciable from the micrographs in Figures 4 and 6. TZM and W showed deformed and elongated grains, with slightly larger grains after the HIP cycle ("H"). This growth was more pronounced for W, and equiaxial microstructure was even observed in Figure 6H, indicating potential recrystallization.

Vickers hardness and thermal conductivity were measured for the four materials after each HIP cycle and are given in Figure 8. The four materials featured slightly lower hardness values for HIP cycle "H," with respect to the hardness values after the HIP cycle "L," with reductions between 10% and 20%. No significant variations of the thermal conductivity were observed for the two HIP cycles.

4 | DISCUSSION

Successful bonding was accomplished for all the target to target material combinations but only when using interfacial aids (Ta interlayer). In these cases, interface microscopy revealed homogeneous and defect-free interfaces.

Due to the difficulties to observe the diffusion layers, the confirmation and extent of diffusion bonding was mainly assessed by the interfacial mechanical strength and thermal conductivity.

High-quality bondings were achieved at the *W*/W and TZM/TZM interfaces, featuring tensile strengths of 215 and 550 MPa respectively and negligible interface thermal resistance.

The HIP parameters did not show significant effects on the bondings but a slight bonding strength reduction was observed for HIP cycle "H." Nevertheless, the use of interfacial aids shows a significant effect in the mechanical strength of the bonding: The strength of the TZM/TZM joint increased from 5 to 550 MPa and that of W/W improved from not bonded to 215 MPa. The significance of the interfacial aid in the resulting bonding strength was already reported for both materials but with different diffusion bonding techniques.[14] The strength of the TZM/TZM joint (550 MPa), which highly exceeds the one of the interlayer material (220 MPa), was attributed to the interlayer's limited plastic flow due to the TZM matrix.[18]

Successful bonding was also achieved between all the combinations of target materials (TZM and W) and cladding materials (Ta and Ta2.5W), and only some difficulties were encountered when bonding W and Ta2.5W with HIP cycle "L." Apart from the latter exception, all the interfaces showed homogeneous morphology without relevant defects. Diffusion bonding extent in the interfaces was evaluated in the same manner as for the target to cladding materials bonding. Nevertheless, diffusion layers with a thickness of approximately 1 μm could eventually be measured, in agreement with literature predictions.[8]

Ta provided satisfactory results as a cladding material, with either TZM or W as target materials, indicating complete diffusion bonding: almost 100% joint efficiency and negligible interface thermal resistance were achieved.

The diffusion bonding of Ta2.5W to TZM was successful in all the cases, obtaining 100% joint efficiency and negligible interface thermal resistance. Nevertheless, Ta2.5W required the use either higher temperature and pressure HIP parameters (cycle "H") or the addition of a Ta interlayer to achieve diffusion bonding with W. With these conditions, 70% joint efficiency and negligible interface thermal resistance were achieved. The difficulties to bond directly W to

Ta2.5W could be attributed to two factors: the higher strength of the Ta2.5W compared with Ta, which limits the material plastic deformation during HIP, or the drop of the diffusion rate due to the small concentration of W in the Ta.[20] This phenomenon was not observed with the TZM as target material, most probably because the increase of the cladding's strength was compensated by the TZM higher ductility.

Contrary to the target to target materials bonding, the HIP cycle parameters clearly affected the bonding properties. With Ta2.5W as a cladding material, using higher T and P (cycle "H") was beneficial to either initiate the bonding or to increase its mechanical strength. Contrarily, with Ta as a cladding material, good mechanical bonding was already achieved with lower T and P (cycle "L"), lower strength was found when using higher T and P (cycle "H"), most probably due to the bulk materials' softening.

In both types of bonding (cladding to target materials and target to target materials), it was found that incipient diffusion bonding is enough to remove the interface's thermal resistance. However, tensile strength of the joints resulted in being more sensitive, hence more indicated to assess the diffusion bonding extent.

A decrease of 10% to 20% in the hardness values was found for the four studied materials after the HIP cycle "H" when comparing with the HIP cycle "L." For the target materials, higher decrease was found for W, most probably due to recrystallisation phenomena (observable in Figure 6H), which starts at lower temperatures than in TZM.

A significant hardness decrease was found for both Ta and Ta2.5W. It could be the cause of the interfacial strength decrease observed in the specimens with Ta as a cladding material, since the tensile strength decrease for the specimens with cycle "H" with respect to the values for cycle "L" corresponds also to 10% to 20%. The diffusion bonding for Ta cladding could be completed with the HIP cycle "L," and the increase of T and P could act only in detriment of the Ta bulk properties. Conversely, the bonding of Ta2.5W would not be completed for HIP cycle "L," and therefore, interfacial strength is increased with the higher T and P from HIP cycle "H." The same reasoning can be expressed for the target to target materials bonding: diffusion bonding with interlayer is already complete with HIP cycle "L" and increasing T and P leads to less strong bonding due to bulk material softening.

5 | CONCLUSIONS

The building of a target block from several target material cylinders bonded together inside the Ta-based cladding was validated. Diffusion bonding assisted by HIP was explored for the first time to self-bond W to W and TZM to TZM downscaled target material cylinders, with promising results. Homogeneous and defect-free interfaces, bonding strengths of 550 and 215 MPa (for TZM-TZM and W-W, respectively) and negligible interface thermal resistance were achieved.

HIP was also proven to be a valid technique to diffusion bond the BDF candidate target materials (W and TZM) to Ta-based erosion-corrosion resistant claddings (Ta and Ta2.5W) in cylindrical geometries representative of the final target. The reported experience in literature was limited to Ta clad W, but in this study, bondings with homogeneous interfaces, 100% joint efficiency and negligible interface thermal resistances were achieved in the combinations Ta-TZM, Ta-W and Ta2.5W-TZM. The same was valid for the combination Ta2.5W-W only with a slightly lower joint efficiency of 70%.

For all the studied bondings, the proper selection of HIP parameters and the use of interfacial aids resulted in being paramount to optimize the interface and the bulk material properties.

Future studies are envisaged to validate the results of this work in up-scaled and eventually beam facing prototypes. As a consequence, upcoming challenges in terms of material procurement, handling and fabrication, and nondestructive examinations will be addressed and developed.

AUTHOR CONTRIBUTIONS

J. Busom Descarrega: Performed the analysis and wrote the paper. T. Hutsch: Collected the data. E. López Sola: Performed the analysis. A.T. Pérez Fontenla: Contributed with data. A. Perillo Marcone: Conceived, designed and performed the analysis. S. Sgobba: Performed the analysis. T. Weißgärber: Conceived and designed the analysis. M. Calviani: Conceived and designed the analysis.

ORCID

Josep Busom Descarrega https://orcid.org/0000-0001-6995-496X
Marco Calviani https://orcid.org/0000-0002-8213-8358
Edmundo López Sola https://orcid.org/0000-0002-9062-4428

Antonio Perillo Marcone https://orcid.org/0000-0002-5826-5074
Stefano Sgobba https://orcid.org/0000-0002-4473-6058

REFERENCES

1. Akmete A, Alexandrov A, Anokhina A, et al. The active muon shield in the SHiP experiment. *Journal of Instrumentation*. 2017;12(05): P05011-P05011. https://doi.org/10.1088/1748-0221/12/05/p05011, https://doi.org/10.1088%2F1748-0221%2F12%2F05%2Fp05011
2. Bonivento W., Boyarsky A., Dijkstra H., Egede U., Ferro-Luzzi M., Goddard B., Golutvin A., Gorbunov D., Jacobsson R., Panman J., et al., Proposal to search for heavy neutral leptons at the SPS, arXiv preprint arXiv:1310.1762.
3. Calviani M. et al., Conceptual design of the SHiP Target and Target Complex, Tech. rep., CERN (2015). URL https://edms.cern.ch/document/1513294/1.0
4. Ishijima Y, Kakiuchi K, Furuya T, et al. Corrosion resistance of refractory metals in high-temperature water. *Journal of Nuclear Materials*. 2002;307–311:1369-1374. https://doi.org/10.1016/S0022-3115(02)01066-8, http://www.sciencedirect.com/science/article/pii/S0022311502010668
5. Lillard R, Pile D, Butt D. The corrosion of materials in water irradiated by 800 MeV protons. *Journal of Nuclear Materials*. 2000;278 (2):277-289. https://doi.org/10.1016/S0022-3115(99)00248-2, http://www.sciencedirect.com/science/article/pii/S0022311599002482
6. Maloy SA, Lillard RS, Sommer WF, et al. Water corrosion measurements on tungsten irradiated with high energy protons and spallation neutrons. *Journal of Nuclear Materials*. 2012) 140–146, Special Issue of the Tenth International Workshop on Spallation Materials Technology, (IWSMT-10). https://doi.org/10.1016/j.jnucmat.2011.11.052, http://www.sciencedirect.com/science/article/pii/S0022311511010075
7. Bermúdez M-D, Carrión FJ, Martínez-Nicolás G, López R. Erosion-corrosion of stainless steels, titanium, tantalum and zirconium. *Wear*. 2005;258(1):693-700, second International Conference on Erosive and Abrasive Wear. https://doi.org/10.1016/j.wear.2004.09.023, http://www.sciencedirect.com/science/article/pii/S004316480400256X
8. Kawai M, Kikuchi K, Kurishita H, Li J-F, Furusaka M. Fabrication of a tantalum-clad tungsten target for kens. *Journal of Nuclear Materials*. 2001;296(1):312-320, 4th Int. Workshop on Spallation Materials Technology. https://doi.org/10.1016/S0022-3115(01)00533-5, http://www.sciencedirect.com/science/article/pii/S0022311501005335
9. Findlay D., ISIS-pulsed neutron and muon source, in: Particle Accelerator Conference, 2007. PAC. IEEE, IEEE, 2007, pp. 695–699.
10. Nelson A, O'Toole J, Valicenti R, Maloy S. Fabrication of a tantalum-clad tungsten target for LANSCE. *Journal of Nuclear Materials*. 2012;431(1–3):172-184.
11. Broome T., Isis target and moderator materials, in: Proceedings of the Second International Workshop on Spallation Materials Technology, No. JUL-3450 in FZJ Report, 1997, pp. 55–59.
12. Gypen L, Brabers M, Deruyttere A. Corrosion resistance of tantalum base alloys. Elimination of hydrogen embrittlement in tantalum by substitutional alloying. *Materials and Corrosion*. 1984;35(2):37-46.
13. Ipatova I, Wady P, Shubeita S, Barcellini C, Impagnatiello A, Jimenez-Melero E. Radiation-induced void formation and ordering in Ta-W alloys. *Journal of Nuclear Materials*. 2017;495:343-350.
14. Metcalfe A., Lindemer T., Diffusion bonding of refractory metals, Tech rep, SOLAR TURBINES INTERNATIONAL SAN DIEGO CA (1963).
15. Kazakov N., Kvasnitsky V., Bonding of refractory and active metals and their alloys, in: Kazakov N. (Ed.), *Diffusion Bonding of Materials*, Pergamon, 1985, pp. 170–186. https://doi.org/10.1016/B978-0-08-032550-7.50013-8. http://www.sciencedirect.com/science/article/pii/B9780080325507500138
16. Li J-F, Kawai M, Kikuchi K, et al. Strength proof evaluation of diffusion-jointed W/Ta interfaces by small punch test. *Journal of Nuclear Materials*. 2003;321(2):129-134. https://doi.org/10.1016/S0022-3115(03)00237-X, http://www.sciencedirect.com/science/article/pii/S002231150300237X
17. Dombrowski D. E., Maloy S. A., Preliminary results for hip bonding Ta to W targets for the materials test station, Tech. rep., Los Alamos National Lab. (LANL), Los Alamos, NM (United States) (2009).
18. Committee A. I. H., Olson D., ASM handbook: welding, brazing, and soldering, ASM Handbook, ASM International, 1993.
19. Martienssen W, Warlimont H. *Springer handbook of condensed matter and materials data*. Springer Science & Business Media; 2006.
20. Tregubov I., Kuzina L., Ivanov O., The interdiffusion of tantalum and tungsten, Tech rep, FOREIGN TECHNOLOGY DIV WRIGHT-PATTERSON AFB OH (1969).

How to cite this article: Busom Descarrega J., Calviani M., Hutsch T., et al. Application of hot isostatic pressing (HIP) technology to diffusion bond refractory metals for proton beam targets and absorbers at CERN, *Mat Design Process Comm*. 2020;2:e101. https://doi.org/10.1002/mdp2.101